Landslides (2010) 7:105–116
DOI 10.1007/s10346-010-0197-9
Received: 10 July 2009
Accepted: 10 January 2010
Published online: 20 February 2010

José Cepeda · José Alexander Chávez · Celina Cruz Martínez

Procedure for the selection of runout model parameters from landslide back-analyses: application to the Metropolitan Area of San Salvador, El Salvador

Abstract The existing procedures for the selection of runout model parameters from back-analyses do not allow integrating different types of runout criteria and generally lack a systematic approach. A new method based on receiver operating characteristic (ROC) analyses and aimed at overcoming these limitations is herein proposed. The method consists of estimating discrete classifiers for every runout simulation associated with a set of model parameters. The set of parameters that yields the best prediction is selected using ROC metrics and space. The procedure is illustrated with the back-analyses of a rainfall-triggered debris flow that killed 300–500 people in the Metropolitan Area of San Salvador in 1982. The selected model parameters are used to estimate forward predictions for scenarios that correspond to different return periods. The proposed procedure may be useful in the assessment of areas potentially affected by landslides. In turn, this information can be used in the production or updating of land use plans and zonations, similar to that currently being carried out by the Office for Urban Planning of the Metropolitan Area of San Salvador in El Salvador.

Keywords Runout model · El Salvador · Landslide · Hazard mapping · Volcanoes · Land-use management

Introduction

The estimation of landslide runout using numerical models is becoming increasingly popular as new models are developed and validated and become readily available in both research and practical applications. The estimation of model parameters can be made by performing laboratory or small-scale experiments in some instances, but there are several cases when the best predictions are achieved using models that cannot be physically reproduced in the laboratory. In such cases, the preferred approach is to perform a calibration of model parameters by carrying out back-analyses of well-documented landslide cases. This paper presents a review of the current procedures for the selection of runout model parameters, emphasising their limitations. A new procedure is proposed based on the receiver operating characteristic (ROC) analyses, and an illustration is presented by applying the method to a rainfall-triggered landslide that killed 300–500 people in the Metropolitan Area of San Salvador in 1982. The parameters calibrated from the back-analyses are used in forward predictions and to produce landslide intensity maps.

Selection of runout model parameters

In landslide risk management, the comparison of the performance of predictive models has advanced significantly in applications of landslide susceptibility assessment. There are several methods to assess statistical performance of susceptibility models: ROC curves (Fawcett 2006), success rate curves, cost curves and total cost curves (Frattini et al. 2008). These methods have been applied in contexts when susceptibility is understood as an "assessment of the classification, volume (or area), and spatial distribution of landslides which exist or potentially may occur in an area" (Fell et al. 2008), but without giving consideration to a description of the velocity and intensity of the existing or potential landsliding.

Fell et al. (2008) define landslide intensity as "a set of spatially distributed parameters related to the destructive power of a landslide. The parameters may be described quantitatively or qualitatively and may include maximum movement velocity, total displacement, differential displacement, depth of the moving mass, peak discharge per unit width, kinetic energy per unit area".

Assessment of landslide intensity using numerical methods requires a selection of runout model parameters. These parameters are normally obtained from back-analyses of relatively well-documented landslide cases.

Existing methods

Three different methods have been applied for the selection of parameters for the estimation of landslide intensity:

a. *Matrix method for comparison of two independent parameters.* This is done by a visual comparison of results of a parametric or sensitivity study (e.g. arranged as a matrix for a two-parameter study; see McDougall 2006; Cepeda 2007; Hungr et al. 2007; Wang and Sassa 2007, among others). As an illustration, in Fig. 1a, the results of simulations using all the possible combinations for parameter values c_1, c_2, c_3, d_1, d_2 and d_3 (brown-filled polygons) are shown superimposed with the observed landslide trail (red polygons). In this hypothetical case, note that parameter c has a control on lateral spread and parameter d on maximum runout. In this example, the calibrated parameters seem to be between c_1 and c_2 and between d_2 and d_3. Three limitations can be identified in this method: (1) The selection relies on a purely graphical and visual estimation (i.e. no quantitative comparisons are performed); (2) it becomes impractical if more than two model parameters need to be calibrated; and (3) it becomes difficult to include other measures of landslide intensity such as maximum velocity, flow depth, kinetic energy, etc.
b. *Maximisation of intersection/union of observed and simulated landslide trails* (Galas et al. 2007; see Fig. 1b). In this method, a ratio "correlation of flow areas" is obtained after dividing the intersection of the observed and simulated flow areas (the method has been applied for landslides of the flow type; Hungr et al. 2001) by the union of both areas. Then, an interpolation procedure can be applied using several combinations of model parameters and their corresponding ratios. After optimisation of the interpolating function, the model parameters that correspond to the maximum ratio "correlation of flow areas"

are obtained. This method overcomes the first and second limitations of method (a), but still shares the third limitation. In addition, this method may assign identical values of the ratio to simulations that yield very different results. For example, (b.1) and (b.2) in Fig. 1 correspond to the same landslide case (the same observed trail represented by the red-outlined cells) but showing results from two different simulations. Note that despite the differences in the simulated results, both cases produce the same value of the ratio (4/24 in (b.1) = 5/30 and in (b.2)=1/6). The ratio "correlation of flow areas" is not able to capture differences due to overpredictions (i.e. amount of simulated results outside the observed trail).

c. *Two-dimensional plot of model parameters* (Hurlimann et al. 2008). This method is similar to method (a) and shares the same limitations. It is based on visual comparisons of velocity profiles and maximum runout between observations and simulated results.

New method

A new method is proposed in order to overcome the limitations presented in the previous section. The proposed method is based on the ROC analysis (Fawcett 2006). In ROC analysis, true class instances (observations) are compared with hypothesised class instances (predictions or simulations) using a classification model (or classifier). The observations are classified in positives or negatives depending on whether they indicate occurrence or non-occurrence of a phenomenon. Predictions are classified as "yes" or "no" depending on whether they occur above or below a threshold for the occurrence of the phenomenon of interest. Table 1 presents the outcomes of a classification model using a confusion matrix. Two important performance metrics that can be calculated from the confusion matrix are the true positive rate, TPR, and the false positive rate, FPR:

$$\mathrm{TPR} = \frac{\mathrm{TP}}{P} \tag{1a}$$

$$\mathrm{FPR} = \frac{\mathrm{FP}}{N} \tag{1b}$$

where all variables are defined in Table 1. Note that values of TPR and FPR range between 0 and 1.

The proposed approach is to estimate discrete classifiers (i.e. pairs of true and false positive rates) from runout simulation results and field observations. The types of criteria should be relevant for the characterisation of runout: flow depth, flow velocity, kinetic energy, impact pressure, maximum runout, area of debris trail, area affected with a certain maximum intensity, etc. ROC metrics can be reformulated as follows for an i-th runout criterion (e.g. maximum velocity, maximum runout, etc.) and a j-th set of runout model parameters (e.g. viscosity and yield strength, friction coefficient and turbulent coefficient):

$$\mathrm{TPR}_{ij} = \frac{\mathrm{TP}_{ij}}{P_i} \tag{2a}$$

$$\mathrm{FPR}_{ij} = \frac{\mathrm{FP}_{ij}}{N_i}. \tag{2b}$$

For each j-th set of runout model parameters, all i-th criteria can be combined by a weighted sum of all the m criteria:

$$\mathrm{TPR}_j = \frac{\sum_{i=1}^{m} \left(w_i \mathrm{TPR}_{ij} \right)}{\sum_{i=1}^{m} w_i} \tag{3a}$$

$$\mathrm{FPR}_j = \frac{\sum_{i=1}^{m} \left(w_i \mathrm{FPR}_{ij} \right)}{\sum_{i=1}^{m} w_i}. \tag{3b}$$

The weights w_i are assigned based on expert judgment about the relative importance of each i-th runout criterion. One possible approach for obtaining the vector of weights w_i is to perform pairwise comparisons between all the m runout criteria and then apply an analytic hierarchy process (Saaty 1977). It is important to note that subjective judgment is introduced in the process of obtaining the weights w_i.

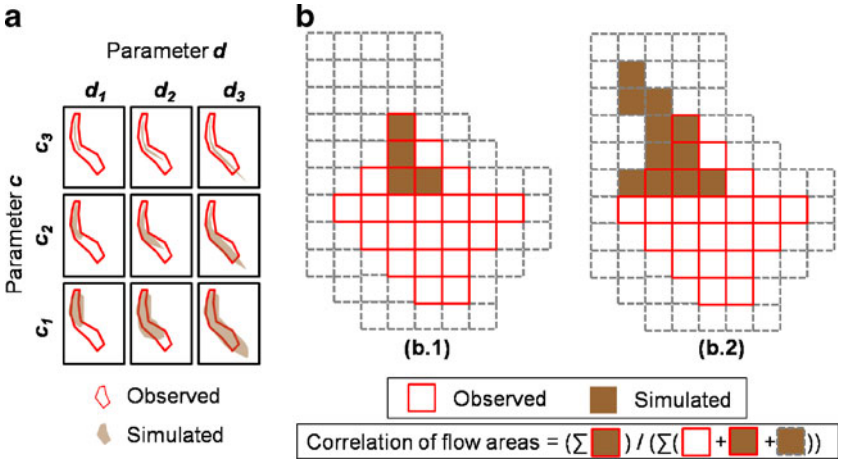

Fig. 1 Methods for calibration of runout model parameters. **a** Matrix method for calibration of two independent parameters. **b** Method of correlation of flow areas

Table 1 Confusion matrix showing outcomes of a classification model (classifier)

		True class (observations)	
		Positives	Negatives
Hypothesized class (predictions or simulations)	"Yes"	True Positives ***TP***	False Positives ***FP***
	"No"	False Negatives ***FN***	True Negatives ***TN***
	Σ	***P***	***N***

Colour filled cells: correct classifications. Hatched cells: incorrect classifications

Finally, the discrete classifiers for each j-th set of runout model parameters are compared in a ROC space by plotting FPR_j in the horizontal axis and TPR_j in the vertical axis, i.e. a point with coordinates (FPR_j, TPR_j). All n combinations of runout model parameters can be compared and a decision can be made based on which j-th set produces the best match with the observations. Three discrete classifiers are important references in the ROC space:

- Maximum underestimation: corresponds to TPR=FPR=0.
- Perfect classification: corresponds to TPR=1 and FPR=0.
- Maximum overestimation: corresponds to TPR=1 and FPR=1.

For a discrete classifier, a norm r_j can be calculated as the distance to perfect classification:

$$r_j = \sqrt{(1 - \mathrm{TPR}_j)^2 + \mathrm{FPR}_j^2}. \quad (4)$$

The predictive performance of two or more sets of runout model parameters can be assessed by comparing their corresponding values of r, TPR and FPR.

The values of the variables on the right-hand side of Eq. 2a and 2b can be estimated as follows:

a. *For single point scalar values* (e.g. maximum velocity, maximum depth, final depth, maximum runout, maximum discharge, etc.). Given an observed value of the i-th criterion uT_i, the positives P_i and negatives N_i are defined in reference to lower- and upper-bound values uL_i and uU_i, respectively (see Fig. 2a.) The lower-bound reference value uL_i corresponds to a lowest intensity reference (e.g. zero velocity and depth). TP_{ij} and FP_{ij} are defined as shown in Fig. 2b, c for simulated values uH_{ij} occurring below and above uT_i, respectively. Two examples of functions for defining the lower- and upper-bound reference values follow:

$$uL_i = \min\left(uH_{ij}\right); uU_i = \max\left(uH_{ij}\right) \quad (5a)$$

$$uL_i = uT_i - \max\left(\left(\max\left(uH_{ij}\right) - uT_i\right), \left(uT_i - \min\left(uH_{ij}\right)\right)\right); \quad (5b)$$

$$uU_i = uT_i + \max\left(\left(\max(uH_{ij}) - uT_i\right), \left(uT_i - \min\left(uH_{ij}\right)\right)\right).$$

In any case, the choice of the lower- and upper-bound reference values should ensure that $0 \le TPR_{ij} \le 1$ and $0 \le FPR_{ij} \le 1$. It should be noted that the bound reference values have influence in stretching the discrete classifiers towards the under- and overestimation ends (i.e. (0,0) and (1,1)) of the ROC space.

b. *For spatially distributed values* (e.g. total impacted area, area with a constant level of maximum observed intensity; see Fig. 2d). P_i is given by the observed area and N_i is a reference area outside the limits of the observed area. N_i can be defined in several ways, for example, by calculating a buffer outside the limits of the observed area, as the maximum extension of an area of interest (e.g. an urbanised area), etc. As in the previous case, the choice for estimating N_i should be such that TPR_{ij} and FPR_{ij} range between 0 and 1. Note that using this method, the

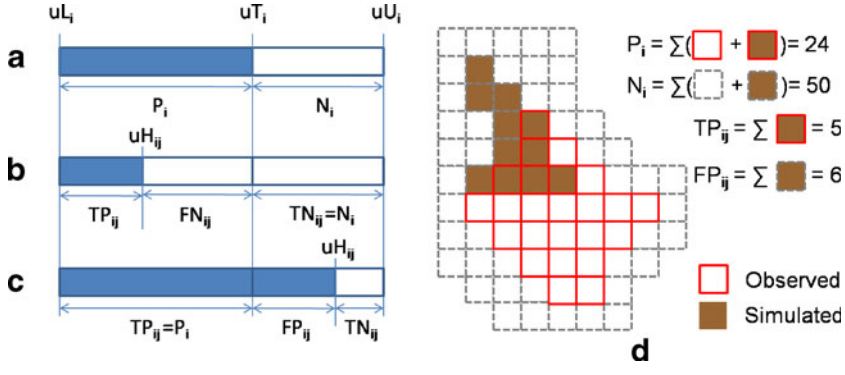

Fig. 2 Definition of variables for estimation of discrete classifiers for single point scalar values (**a**–**c**) and for spatially distributed values (**d**)

cases in b.1 and b.2 in Fig. 1 are distinguishable since they map different points in the ROC space: (0, 0.167) and (0.120, 0.208), respectively.

The following section presents an illustration of this new method for the selection of runout model parameters.

Application to the AMSS, El Salvador

The Metropolitan Area of San Salvador (AMSS) is constituted by 14 municipalities including the capital city of El Salvador. The AMSS concentrates around one third of the population of El Salvador in an area severely hit by several types of natural hazards, namely earthquakes, floods, landslides and volcanic eruptions. The impact as a consequence of natural hazards in El Salvador is high, partly due to the level of exposure connected with a high concentration of population (288 inhabitants per square kilometre), making it the most densely populated country in the American continent and the ninth worldwide among countries having an area >20,000 km² (data.un.org).

As an example of the impact due to recent natural hazards in El Salvador, landslides induced by the 2001 earthquakes accounted for 92% of the total losses in the infrastructure sector and demanded 100% of the restoration costs in connection with environmental damages (Zapata Martí and Jovel 2004). Around 70% of the ~900 casualties of the 13 January 2001 earthquake in El Salvador were produced by a single landslide in the Las Colinas neighbourhood in the AMSS (Crosta et al. 2005; Orense et al. 2002).

Context of highly mobile landslides

In the AMSS, landslides with high mobility (i.e. high velocities and long runout distances) occur in connection with earthquake and rainfall triggering factors. A shallow-focus earthquake in 1986 triggered several liquefaction-initiated landslides in the epicentral area within the AMSS (Rymer 1987), and the 13 January 2001 earthquake triggered the infamous Las Colinas landslide that killed more than 600 people in a neighbourhood at the southwest of the AMSS. Risk levels have been controlled in that area after mitigation works were carried out and reoccupation of the impacted area was banned by the authorities.

Rainfall-triggered landslides also impose a significant threat in the AMSS, producing devastating consequences. A debris flow in September 1982 was initiated on the upper slopes of the El Picacho peak on the edifice of the San Salvador volcano and killed an estimated of 300–500 persons in a neighbourhood to the northwest of the AMSS. That same area had been hit by a larger debris flow in 1934, but without causing any consequences to life or property since the zone was not inhabited at that time. In October 2008, a rainfall-triggered small debris flow occurred in the same catchment of the 1982 event, but due to the relatively small volume involved (~3,000 m³), it had a short runout distance that did not reach any populated or built areas. Currently, there is considerable concern in the Salvadoran authorities regarding the design and implementation of measures for risk reduction in the areas surrounding the El Picacho peak, partly due to the pressure from the local residents, the media and the general public. One of the measures that are required is the updating of the zonation maps that are used for urban planning. The present section of this paper is aimed at producing simulations of landslide scenarios that can be used for the updating of such maps. The simulations use runout model parameters calibrated using the new procedure introduced in the previous section.

Back-analyses

The 1982 landslide at the El Picacho was triggered in connection with an intense and prolonged period of precipitation from 17 to 19 September. The landslide was initiated before 6:00 A.M. on 19 September on the upper slopes on the eastern side of the El Picacho peak and within the Las Lajas ravine. El Picacho is entirely composed of volcanic rocks that consist of fractured lava flows intercalated with tephra deposits (pyroclastic soils). The upper slopes are intensively weathered to a maximum depth of 5–10 m (Sebesta 2007). The landslide source area was located between 1,600 and 1,925 m.a.s.l. An estimated volume of 425,000 m³ of material ruptured over an area of ~60,700 m² with an average depth of the rupture surface of 7 m in the source area (Kiernan and Ledru 1996). The landslide material was transformed into a debris flow that travelled a distance of ~4 km, reaching several neighbourhoods at an elevation of ~750 to 800 m.a.s.l. where it caused numerous casualties and damage over an impact area of ~97,000 m² (Bäcklin and Finnson 1994). Figure 3 is an aerial photo of the El Picacho showing the debris trail of the 1982 landslide. Sites A and B in Fig. 3 mark the crown of the scarp and the mid-height of the release area, respectively.

Samples of the debris flow were retrieved from the only remaining deposit located on a park on the northern bank of the Las Lajas ravine (site C in Fig. 3). Our observations and the available reports for this case do not give indications whether there was notable variation in the characteristics of the debris in different parts of the runout trail. Figure 4 shows a grain size distribution of the samples (curves with markers). For reference, the lower and upper bound of samples from similar pyroclastic debris flows in Campania, Italy are also shown (Revellino et al. 2004). As the curves indicate, the fine content of the debris flow deposit is <10% with a predominant sand fraction ranging from

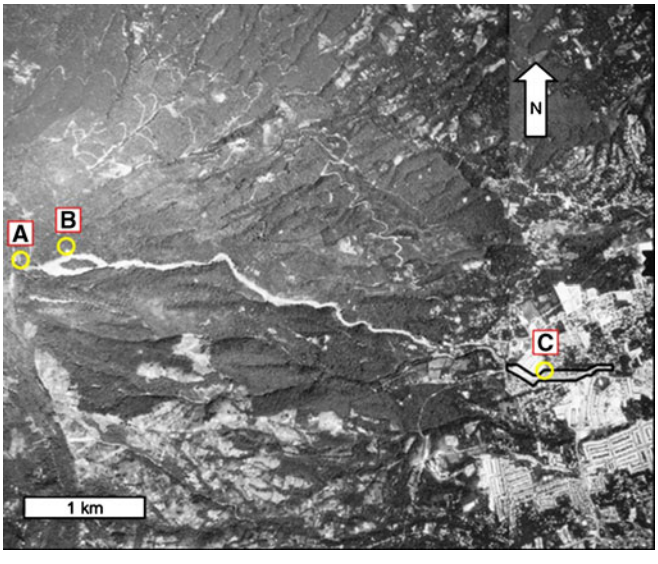

Fig. 3 Aerial photo showing the trail of the 1982 debris flow. **a** Crown of the release area. **b** Marks the mid-height of the rupture area. **c** Deposition area where samples were retrieved

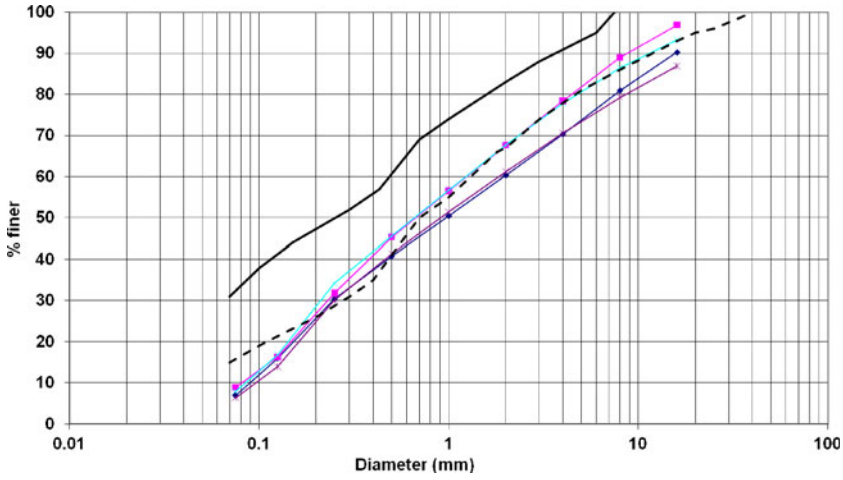

Fig. 4 Grain size distribution of samples retrieved from debris flow deposit (*curves with markers*) and lower and upper bound (*dashed* and *solid thick black lines*) of debris flow samples in Revellino et al. (2004)

60% to 70% in weight. Atterberg limits were estimated to be 37 and 31 for the liquid and plastic limit, respectively, indicating a non-plastic silt.

The release area has been defined based on the description by Kiernan and Ledru (1996) and is shown as the red polygon to the left on Fig. 5. The digital elevation model is a 10-m grid prepared based on 10-m contours obtained from 1:25,000 topographic maps produced in 1984.

The Voellmy model has proved to be adequate for the simulation of debris flows containing pyroclastic soils (McDougall 2006; Revellino et al. 2004) and is here used for back-analyses of the 1982 landslide. A simple formulation of the Voellmy model is:

$$\tau = \mu\sigma + \frac{\gamma v^2}{\xi} \tag{5}$$

where τ is the bed shear stress, σ is the bed normal total stress, μ is the friction coefficient, γ is the unit weight of the flowing mass, v is the depth-averaged flow velocity and ξ is the turbulent coefficient.

The runout model that is used for the back-analyses and the forward predictions is the DAN3D model (McDougall and Hungr

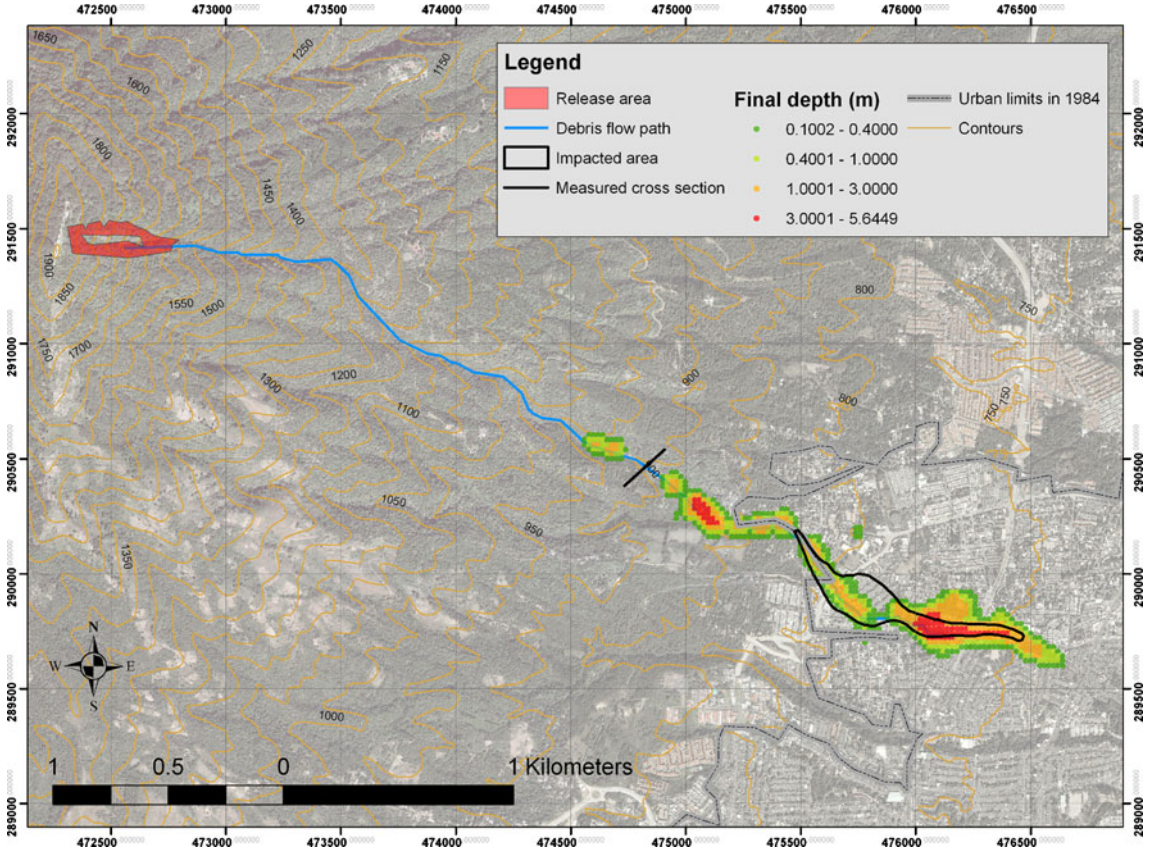

Fig. 5 Final simulated deposit of 19 September 1982 debris flow. Parameters of Voellmy model are μ=0.05 and ξ=500 m/s^2

Table 2 Sets of model parameters used for back-analyses of the 1982 landslide at the El Picacho peak

		Turbulent coefficients (m/s^2)		
		Set A: 200	Set B: 500	Set C: 1,000
Friction coefficients	Set 1: 0.05	1A	1B	1C
	Set 2: 0.07	2A	2B	2C
	Set 3: 0.11	3A	3B	3C

2004). DAN3D is based on a Lagrangian formulation that discretises the landslide mass in a number of particles representing bed-normal columns of flow. The values of the field variables for each particle are calculated at each time step using an interpolation technique based on smoothed particle hydrodynamics (Gingold and Monaghan 1977; Lucy 1977). The internal stresses are functions of the internal shear strains and are bounded by active and passive states. Voellmy is one of the available models that DAN3D incorporates for calculating the shear stresses at the contact between the landslide mass and the bed.

Based on the ranges of parameter values used by McDougall (2006) and Revellino et al. (2004), nine sets of model parameters have been used in simulations for the back-analyses of the 1982 landslide. The value of the friction coefficient is varied from 0.05 to 0.11 and the turbulent coefficient from 200 to 1,000 m/s^2. The values of the nine sets of model parameters are defined according to Table 2.

Illustration of new method for selection of runout model parameters

The following eight runout criteria are used for comparing simulations and field observations:

- Criterion 1: maximum runout. This is the longitude coordinate of the maximum observed runout based on the impact area mapped by Bäcklin and Finsson (1994). It is equal to 476,468 m.
- Criterion 2: impact area. This is the area of the observed impact zone in the affected neighbourhoods (see black polygon on the right in Fig. 5). It is equal to 97,197 m^2.
- Criterion 3: maximum cross-sectional area at the runout trail. This is the maximum cross-section area at a channel section located at a latitude of ~290,500 m (see black line crossing the debris trail in Fig. 5). Based on field observations, a topographic survey and interviews with witnesses of the 1982 debris flow, Blanco et al. (2002) estimated the area of this cross-section as 150 m^2.
- Criteria 4 and 5: final and maximum flow depths at landslide deposit (currently, a park) shown as zone C in Fig. 3. These depths values were measured on site or obtained from witness reports. The final depth has been obtained by measuring the thickness of the deposit in a post-landslide inspection and is equal to 1.5 m. The maximum flow depth was assessed based on witnesses reports found in contemporary newspapers and is equal to 2 m.
- Criteria 6, 7 and 8: final and maximum flow depths and maximum velocity at a pink house, also in zone C as shown in Fig. 3, which is about 100 m to the south of the park that was referred to in criteria 4 and 5. The final depth (1 m) and maximum velocity (4.4 m/s) were estimated based on photos published in contemporary newspapers. The maximum velocity was calculated by measuring the height of run-up using the mud splash marks on the walls of one of the few houses that was not destroyed by the flow. As in criterion 5, the maximum flow depth was set to be equal to 2 m based on contemporary press reports.

In order to illustrate the calculation procedure of the discrete classifiers, some examples are presented using the set of model parameters 2B in Table 2 (this corresponds to row $j=5$ in Table 3). These examples correspond to the calculations required to obtain the values in bold cells in Table 3:

- Runout criterion $i=1$: longitude coordinate of maximum runout.

The maximum simulated runout is 476,190 m; hence, $uH_{1,5}=$ 476,190 m.

Since $uH_{1,5}<uT_1=476{,}468$ m (see fourth row in Table 3), then this case corresponds to Fig. 2b.

Table 3 Estimation of discrete classifiers for the back-analyses of the 1982 landslide at the El Picacho peak on the San Salvador volcano using the sets of model parameters of Table 2 and the proposed method described in "New method" of this paper

i (runout criterion)→	1		2		3		4		5		6		7		8		TPR_j	FPR_j
w_i→	2		3		1		1		1		1		1		1			
Criterion→	Longitude coordinate of Max. runout		Impact area		Trail cross-section		Depth at park		Max. depth at park		Depth at pink house		Max. depth at pink house		Max. Vel. at pink house			
uT_i →	476,468 m		97,197 m^2		150 m^2		1.5 m		2 m		1 m		2 m		4.4 m/s			
j (set of model parameters) ↓	TPR_{1j}	FPR_{1j}	TPR_{2j}	FPR_{2j}	TPR_{3j}	FPR_{3j}	TPR_{4j}	FPR_{4j}	TPR_{5j}	FPR_{5j}	TPR_{6j}	FPR_{6j}	TPR_{7j}	FPR_{7j}	TPR_{8j}	FPR_{8j}		
1 (1A)	1	1	0.889	0.126	1	0.772	0.4	0	1	0.091	0.8	0	1	0.722	0.955	0	0.893	0.360
2 (1B)	1	0.336	0.901	0.206	1	1	0.4	0	0.65	0	0.9	0	1	0.278	0.841	0	0.863	0.234
3 (1C)	1	0	0.840	0.236	1	0.584	0.2	0	0.4	0	0.4	0	0.75	0	1	0	0.752	0.118
4 (2A)	0.956	0	0.584	0.066	1	0.370	1	1	1	1	1	1	1	1	0.636	0	0.846	0.415
5 (2B)	**0.683**	**0**	**0.539**	**0.087**	1	0.925	1	0.167	0.8	0	**1**	**0.462**	1	0.222	0.636	0	0.765	**0.185**
6 (2C)	0.456	0	0.193	0.068	1	0.677	0.267	0	0.2	0	0.7	0	0.35	0	0.705	0	0.428	0.080
7 (3A)	0.251	0	0.152	0.029	1	0.541	0	0	0	0	0	0	0	0	0	0	0.178	0.057
8 (3B)	0.137	0	0.086	0.025	1	0.463	0	0	0	0	0	0	0	0	0	0	0.139	0.049
9 (3C)	0	0	0.016	0.006	1	0.477	0	0	0	0	0	0	0	0	0	0	0.095	0.045

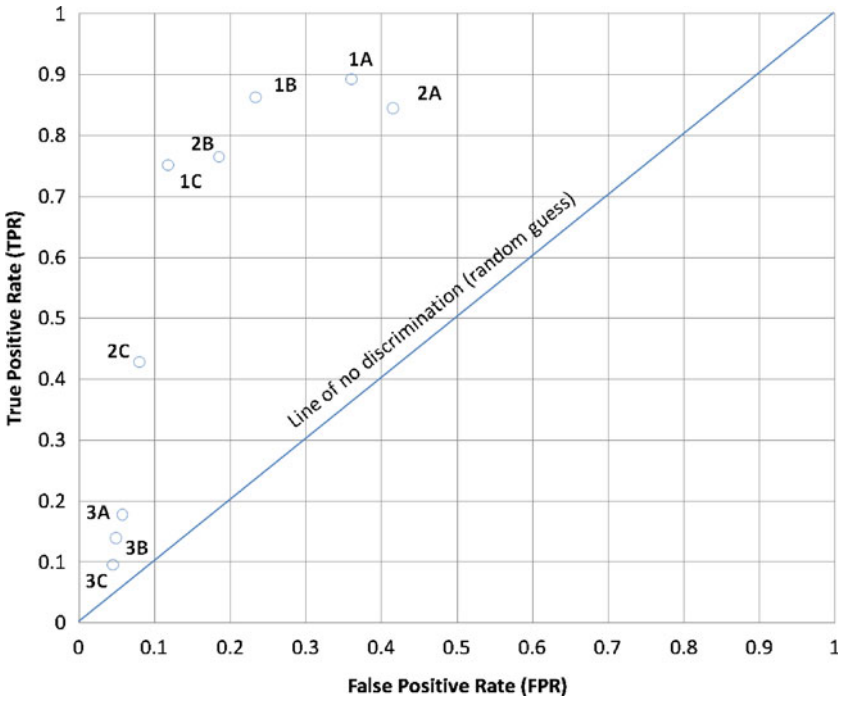

Fig. 6 Discrete classifiers for the nine combinations of Voellmy model parameters plotted in the ROC space. The *number in each marker label* identifies the friction coefficient and the *letter* the turbulent coefficient. Numbers *1*, *2* and *3* correspond to friction coefficients of 0.05, 0.07 and 0.11. Letters *A*, *B* and *C* correspond to turbulent coefficients of 200, 500 and 1,000 m/s^2

Using Eq. 5a, uL_1=475,590 m (equal to $uH_{1,9}$, which produces the lowest prediction of maximum runout, and accordingly $TPR_{1,9}$=0).

Then, according to Fig. 2b, $TP_{1,5}=uH_{1,5}-uL_1$=476,190–475,590=600 m.

And according to Fig. 2a, $P_1=uT_1-uL_1$=476,468–475,590=878 m.

Finally, applying Eq. 2a yields:

$$TPR_{1,5} = TP_{1,5}/P_1 = 600\,\text{m}/878\,\text{m} = 0.683.$$

From Fig. 2b, note that $FP_{1,5}$=0; hence, $FPR_{1,5} = 0$. In fact, note that for all cases that correspond to Fig. 2b, $FPR_{i,j}$ is always equal to 0.

- Runout criterion i=2: impact area.

The simulated impact area occurring within the observed impact area is 52,400 m^2. This corresponds to $TP_{2,5}$ according to Fig. 2d; hence, $TP_{2,5}$=52,400 m^2.

The observed impact area is P_2=97,197 m^2 (see fourth row in Table 3).

Then, applying Eq. 2a yields:

$$TPR_{2,5} = TP_{2,5}/P_2 = 52,400\,\text{m}^2/97,197\,\text{m}^2 = 0.539.$$

The simulated impact area occurring outside the observed impact area is 47,200 m^2. This corresponds to $FP_{2,5}$ according to Fig. 2d; hence, $FP_{2,5}$=47,200 m^2.

A reference area outside the impact area has been obtained by creating a buffer around the black polygon shown in Fig. 5. This reference area is equal to N_2=544,861 m^2 (see Fig. 2d).

Finally, applying Eq. 2b yields:

$$FPR_{2,5} = FP_{2,5}/N_2 = 47,200\,\text{m}^2/544,861\,\text{m}^2 = 0.087.$$

- Runout criterion i=6: depth at pink house.

The final simulated depth at the pink house is 2.2 m; hence, $uH_{6,5}$=2.2 m.

Since $uH_{6,5} > uT_6$=1 m (see fourth row in Table 3), then this case corresponds to Fig. 2c.

Table 4 Scenarios for forward predictions of debris flows initiating at the El Picacho peak on the San Salvador volcano

Scenario	Catchment	Ravine	Slope in rupture area (deg)	Average depth of rupture (m)	Area of landslide source (m^2)	Volume of debris flow (m^3)	Return period (years)
1_lowfrq	1	Las Lajas (Mejicanos)	≥35	7	100,400	702,800	>92
1_highfrq	1	Las Lajas (Mejicanos)	≥40	1.5	39,200	58,800	27 to 92
2_lowfrq	2	La Quebradona and El Muerto	≥35	7	424,800	2,973,600	>92
2_highfrq	2	La Quebradona and El Muerto	≥40	1.5	180,800	271,200	27 to 92
3_lowfrq	3	Las Lajas (Escalón)	≥35	7	54,800	383,600	>>92
3_highfrq	3	Las Lajas (Escalón)	≥40	1.5	27,200	40,800	>92

Table 5 Cutoff and boundary values of flow depths and velocities

	Cutoff values	Boundary values
Flow depth (m)	0.1 (approximate cutoff value; Bureau of Reclamation 1988; FLO-2D 2004)	0.4, 1 (Rickenmann 2005)
		1, 3 (KWL Ltd 2003)
Flow velocity (m/s)	0.05 (limit between rapid and very rapid landslides; Cruden and Varnes 1996)	0.4, 1.5 (Rickenmann 2005)
		3 (KWL Ltd. 2003; Varnes 1978)
		5 (Cruden and Varnes 1996)

Using Eq. 5a, uU_6=3.6 m (equal to $uH_{6,4}$, which produces the highest prediction of final depth at the pink house, and accordingly $TPR_{6,4}=FPR_{6,4}=1$).

Then, according to Fig. 2c, $FP_{6,5}=uH_{6,5}-uT_6=2.2-1=1.2$ m.

And according to Fig. 2a, $N_6=uU_6-uT_6=3.6-1=2.6$ m.

Finally, applying Eq. 2b yields:

$$FPR_{6,5} = FP_{6,5}/N_6 = 1.2\,\text{m}/2.6\,\text{m} = 0.462.$$

From Fig. 2c, note that $TP_{6,5}=P_6$; hence, $TPR_{6,5} = 1$. In fact, note that for all cases that correspond to Fig. 2c, $TPR_{i,j}$ is always equal to 1.

- Calculation of FPR_5.

Expanding Eq. 3b for j=5 and m=8:

$$FPR_5 = \frac{w_1 FPR_{1,5} + w_2 FPR_{2,5} + \ldots + w_7 FPR_{7,5} + w_8 FPR_{8,5}}{w_1 + w_2 + \ldots + w_7 + w_8}.$$

And after substituting the corresponding values from row j=5 in Table 3:

$$FPR_5 = \frac{(2)(0) + (3)(0.087) + (1)(0.925) + (1)(0.167) + (1)(0) + (1)(0.462) + (1)(0.222) + (1)(0)}{2+3+1+1+1+1+1+1}$$

$$FPR_5 = \frac{2.037}{11} = 0.185.$$

In a similar way, Table 3 is completed for all the runout criteria and the sets of model parameters. The discrete classifiers calculated for each set of model parameters are listed in the last two columns of Table 3. Finally, the discrete classifiers plotted in the ROC space are shown in Fig. 6. Each set of model parameters is identified using the code described in Table 2. It should be noted that if it is given sole consideration of the "impact area" runout criterion (i=2 in Table 3), the outcome of this method can be equivalent to the matrix method described in "Existing methods".

In Fig. 6, the three discrete classifiers that are closest to the point of perfect classification (0,1) correspond to sets 1B, 1C and 2B. Among these three sets, the set yielding the highest true positive rate is 1B, which is chosen as the set of runout model parameters that are used for the forward predictions in the next section. Set 1B corresponds to a friction coefficient of 0.05 and a turbulent coefficient of 500 m/s^2. As a comparison, the sets of parameters calibrated by Revellino et al. (2004) ranged from 0.05 to 0.11 for the friction coefficient, and a constant value of 200 m/s^2 was used for the turbulent coefficient. The differences in turbulent coefficient can be attributed to a behaviour tending to a more purely frictional behaviour in the San Salvador debris flow compared to the Campania events. This can be supported by the grain size distribution curves in Fig. 4 which indicate a lower fine fraction (i.e. higher coarse fraction) in the San Salvador deposits than in the Campania sediments.

The distribution of final simulated depths for the back-analyses using set 1B is shown in Fig. 5.

Forward predictions

The calibrated runout model parameters selected in the previous section are used to estimate forward predictions for scenarios resulting from the combination of the following criteria:

a. Landslide source areas at the upper slopes of the Las Lajas ravine (at the Mejicanos municipality), hereafter referred to as "catchment 1"; the La Quebradona and El Muerto ravines, referred to as "catchment 2"; and the Las Lajas ravine (at the Escalón neighbourhood), referred to as "catchment 3".
b. Landslide source areas located within zones of intensive weathering reaching depths between 5 and 10 m.

Table 6 Definition of landslide intensity levels based on maximum velocities and maximum depths

	v_{max}<1.5 m/s	1.5 m/s≤v_{max}<3 m/s	v_{max}≥3 m/s
h_{max}≥3 m	High	High	High
1 m≤h_{max}<3 m	Medium	Medium	High
0.4 m≤h_{max}<1 m	Low	Medium	Medium
h_{max}<0.4 m	Low	Low	Low

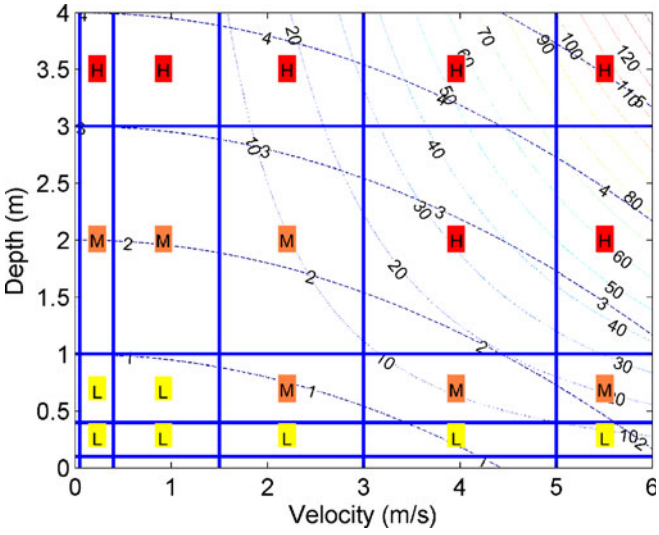

Fig. 7 Definition of intensity levels as a combination of depth and velocity. For reference, two sets of curves are shown: contours of constant specific energy ($v^2/2g+h$) in metres (concave down *dashed curves*) contours of constant v^2h (i.e. linearly proportional to impact force) in cubic metre per second (concave up *dotted curves*). *Vertical* and *horizontal blue thick lines* are reference or boundary values of depth and velocity defined by several authors (see Table 5)

c. Frequency of occurrence. "High frequency" (steep slopes and shallow ruptures): slopes ≥40° and depth of rupture=1.5 m. "Low frequency" (moderately steep and steep slopes and deep ruptures): slopes ≥35° and depth of rupture=7 m.

The above assumptions have been defined based on field observations of previous instabilities and on the report prepared by Sebesta (2007) for the Office for Urban Planning of the Metropolitan Area of San Salvador.

The six scenarios for forward predictions are presented in Table 4.

Landslide intensity maps

The combination of flow velocities v and depths h is a common approach for the estimation of levels of landslide intensities. This is based on the dependence of constant specific energy ($v^2/2g+h$) and impact force (linearly proportional to v^2h). Several cutoff and boundary values of depths and velocities can be drawn from the literature (e.g. see Table 5).

Table 6 and Fig. 7 show the classification of levels of landslide intensities that are used in the present study.

The simulated flow depths and velocities that result from the six scenarios in Table 4 are processed using raster algebra to obtain levels of landslide intensities according to the criteria presented in Table 6 and Fig. 7.

The landslide intensity maps for the six scenarios are presented in Figs. 8 and 9. For reference, these figures also include polygons and lines identifying the trails of the 1982 and 2008 landslides (labelled as "DF 1982" and "DF 2008", respectively) and of a hyperconcentrated flow (labelled as "HCF 2004") that occurred in 2004 and initiated due to erosion and bulking in burned areas.

Discussion of practical aspects

In the application presented in "Application to the AMSS, El Salvador", the calibration of model parameters was done for a single landslide case. Furthermore, the observed values of runout criteria were considered as values without an associated uncertainty and error. Based on these aspects, and with the perspective of a more generalised application of the method, the following practical situations are briefly discussed:

a. *Calibration for a set of landslide cases.* In landslide hazard assessments at a regional scale, the calibration of runout model parameters has to be carried out using sets of cases which are grouped based on some common features (e.g. type of landslide or material, range of volumes). In such conditions, a k-th landslide case within a set of p cases has a discrete classifier (FPR_j^k, TPR_j^k) and a norm r_j^k for the j-th set of runout model parameters. Then, using all p landslide cases, it is possible to calculate the location parameters (e.g. the mean values) of FPR, TPR and r for each j-th set of parameters. These location parameters can be denoted as $E[FPR_j]$, $E[TPR_j]$ and $E[r_j]$, respectively. Finally, the discrete classifiers ($E[FPR_j]$, $E[TPR_j]$) can be plotted for all n sets of model parameters and can be used in combination with the corresponding values of $E[r_j]$ to select the set of runout model parameters with the best predictive performance.
b. *Uncertainty in the observed runout criteria.* In a general case, the observed values of runout criteria uT_i can be characterised as random variables. In such situation, the performance of the j-th set of model parameters cannot be adequately represented as a discrete classifier (FPR_j, TPR_j) on the ROC space. Instead, a probability mass function (PMF) or a probability density function (PDF) in terms of FPR and TPR should be generated based on the probability distribution of uT_i. Once the PMF or PDF have been obtained for a j-th set of model parameters, the first moments of the probability distribution with respect to the point of perfect classification (0,1) or to the origin axes can be used to assess the predictive performance of each set of runout model parameters.

Conclusions

- A method has been proposed to allow comparisons between simulations of runout models and field observations using ROC analyses.
- The method facilitates the combination of different types of runout criteria.
- Cases that become indistinguishable with the existing approaches can be clearly identified and differentiated using the new method.
- The selection of runout model parameters using back-analyses is performed by applying an approach that is more comprehensive than the existing procedures. Some subjective judgment is introduced in the method during the process of obtaining weights for each runout criterion.
- Back-analyses of a catastrophic debris flow in the AMSS in 1982 were performed using sets of runout model parameters drawn from experiences in similar settings.
- The selection of model parameters for the simulation of forward predictions of rainfall-induced debris flows in the AMSS was performed using the new proposed method.

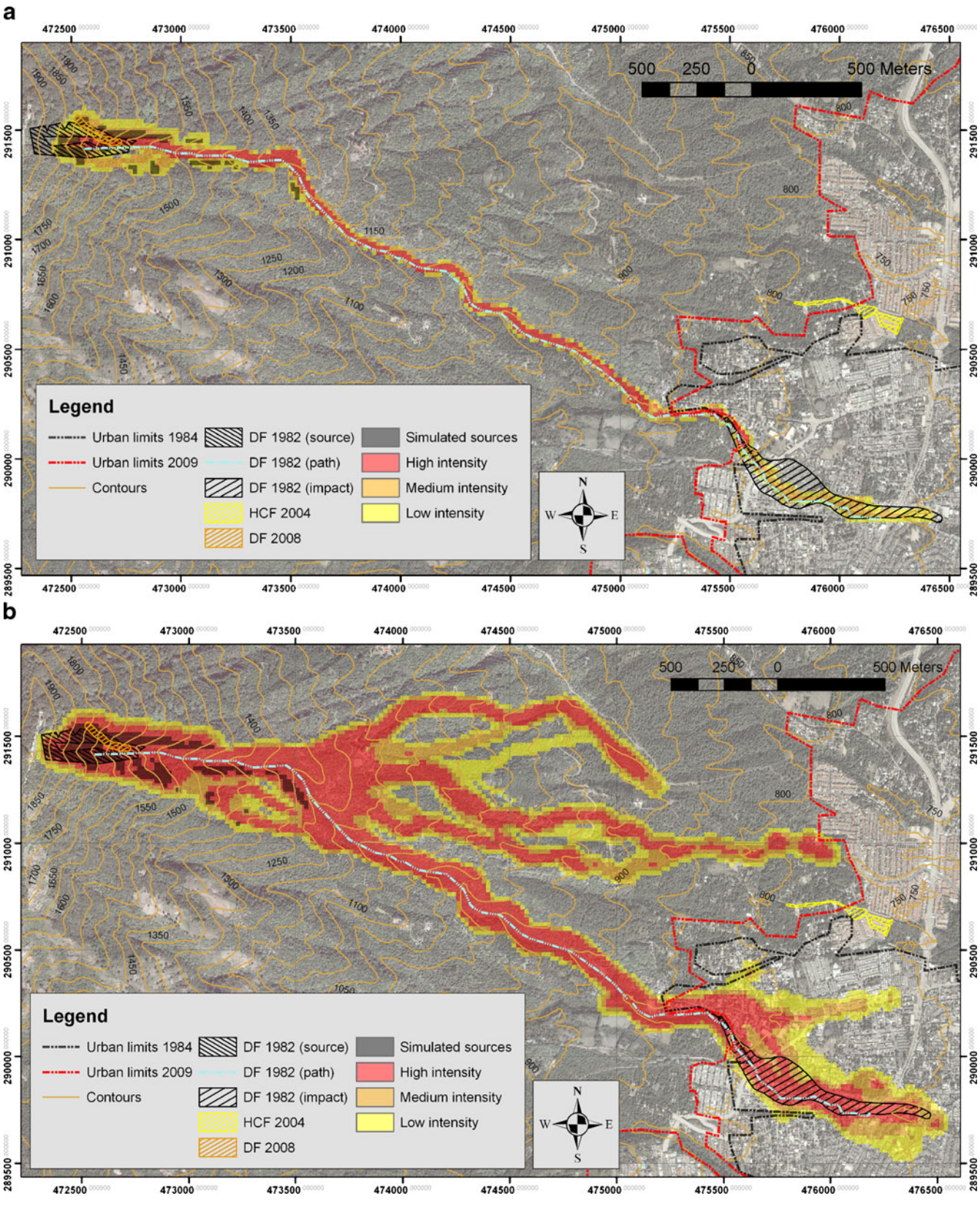

Fig. 8 Simulated intensities for debris flows on catchment 1 released from weathered areas having: **a** slope angles ≥40° and thickness equal to 1.5 m, **b** slope angles ≥35° and thickness equal to 7 m

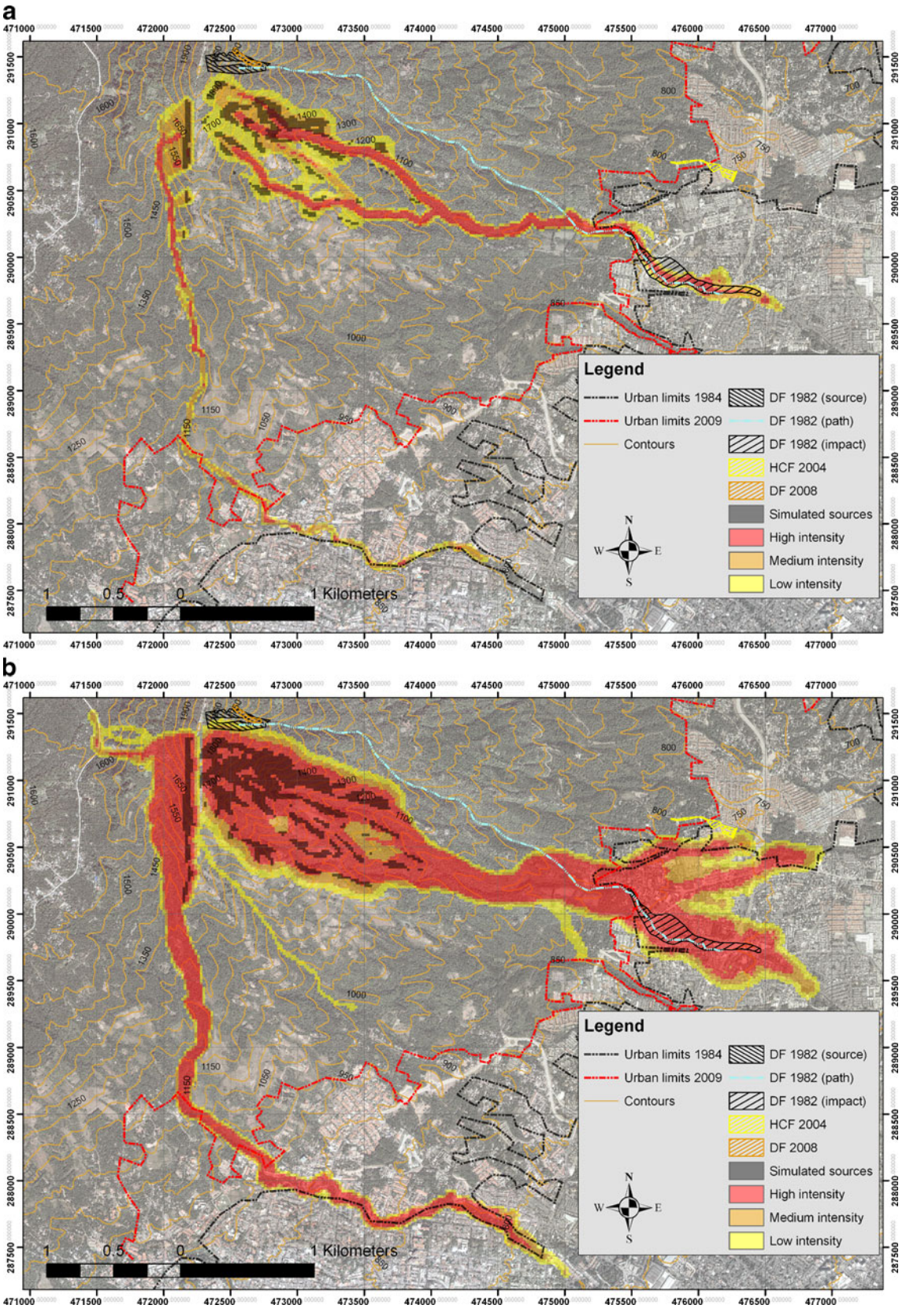

Fig. 9 Simulated intensities for debris flows on catchments 2 (eastern flank) and 3 (western flank) released from weathered areas having: **a** slope angles ≥40° and thickness equal to 1.5 m, **b** slope angles ≥35° and thickness equal to 7 m

Acknowledgements

The contributions of the following persons and institutions are gratefully acknowledged: Prof. Oldrich Hungr (University of British Columbia) who kindly provided a beta version of DAN3D to the Norwegian Geotechnical Institute (NGI) and the International Centre for Geohazards (ICG); Faculty and Staff at the Department of Structural Mechanics at Universidad Centroamericana "José Simeón Cañas", San Salvador for support with field work and laboratory tests; Manuel Díaz (Servicio Nacional de Estudios Territoriales, SNET) and Carlos Pullinger (LaGeo) for their support during field work and for fruitful discussions that have provided useful insight; and Giovanni Molina (Servicio Nacional de Estudios Territoriales, SNET) for providing the digital elevation maps that were used in the simulations. The comments from H. Wing Sun and an anonymous reviewer are greatly appreciated for their contribution in improving this manuscript. This study was financed by the Research Council of Norway through the International Centre for Geohazards (ICG), and the Quota Scheme of the Norwegian State Educational Loan Fund. Their support is gratefully acknowledged. This is ICG article no. 267.

References

Blanco FA, Burgos EA, Mejía M (2002) Estudio de amenazas por lahar en El Salvador: revisión de casos históricos y calibración de herramientas para la evaluación de amenaza. Senior thesis, Universidad Centroamericana, San Salvador, 158 pp

Bureau of Reclamation (1988) Downstream hazard classification guidelines. Acer Technical Memorandum No. 11, Denver, Colorado, USA

Bäcklin C, Finnson H (1994) Landslide hazard at the San Salvador volcano. Royal Institute of Technology, Stockholm, Sweden, p 136

Cepeda J (2007) The 2005 Tate's Cairn debris flow: back-analysis, forward predictions and a sensitivity analysis. In: Ho K, Li V (eds) 2007 International Forum on Landslide Disaster Management. Geotechnical Division, The Hong Kong Institution of Civil Engineers, Hong Kong, pp 813–833

Crosta GB, Imposimato S, Roddeman D, Chiesa S, Moia F (2005) Small fast-moving flow-like landslides in volcanic deposits: the 2001 Las Colinas Landslide (El Salvador). Eng Geol 79(3–4):185–214

Cruden DM, Varnes DJ (1996) Landslide types and processes. In: Turner AK, Schuster RL (eds) Landslides: investigation and mitigation. Transportation Research Board, National Research Council, Washington, DC, USA, pp 36–75

Fawcett T (2006) An introduction to ROC analysis. Pattern Recogn Lett 27(8):861–874

Fell R et al (2008) Guidelines for landslide susceptibility, hazard and risk-zoning for land use planning. Eng Geol 102(3–4):85–98

FLO-2D (2004) FLO-2D users manual version 2004.10. FLO-2D Software, Inc., Nutrioso, Arizona, USA

Frattini P, Crosta GB, Carrara A (2008) Techniques for the evaluation and comparison landslide susceptibility models. European Geosciences Union General Assembly, Vienna

Galas S, Dalbey K, Kumar D, Patra A, Sheridan M (2007) Benchmarking TITAN2D mass flow model against a sand flow experiment and the 1903 Frank slide. In: Ho K, Li V (eds) 2007 International Forum on Landslide Disaster Management. Geotechnical Division, The Hong Kong Institution of Civil Engineers, Hong Kong, pp 899–917

Gingold RA, Monaghan JJ (1977) Smoothed particle hydrodynamics—theory and application to non-spherical stars. Mon Not Roy Astron Soc 181(2):375–389

Hungr O, Evans SG, Bovis MJ, Hutchinson JN (2001) A review of the classification of landslides of the flow type. Environ Eng Geosci 7(3):221–238

Hungr O, McKinnon M, McDougall S (2007) Two models for analysis of landslide motion: application to the 2007 Hong Kong benchmarking exercises. In: Ho K, Li V (eds) 2007 International Forum on Landslide Disaster Management. Geotechnical Division, The Hong Kong Institution of Civil Engineers, Hong Kong, pp 919–932

Hurlimann M, Rickenmann D, Medina V, Bateman A (2008) Evaluation of approaches to calculate debris-flow parameters for hazard assessment. Eng Geol 102(3–4):152–163

Kiernan SH, Ledru O (1996) Remedial measures against landslide hazards at the San Salvador volcano, El Salvador. Royal Institute of Technology, Stockholm, Sweden 100 pp

KWL Ltd (2003) Debris flow study and risk mitigation alternatives for Percy Creek and Vapour Creek (Final Report, December), District of North Vancouver, Canada

Lucy LB (1977) Numerical approach to testing of fission hypothesis. Astron J 82 (12):1013–1024

McDougall S (2006) A new continuum dynamic model for the analysis of extremely rapid landslide motion across complex 3D terrain. PhD thesis, University of British Columbia, Vancouver, 268 pp

McDougall S, Hungr O (2004) A model for the analysis of rapid landslide motion across three-dimensional terrain. Can Geotech J 41(6):1084–1097

Orense R, Vargas-Monge W, Cepeda J (2002) Geotechnical aspects of the January 13, 2001 El Salvador earthquake. Soils Found 42(4):57–68

Revellino P, Hungr O, Guadagno FM, Evans SG (2004) Velocity and runout simulation of destructive debris flows and debris avalanches in pyroclastic deposits, Campania region, Italy. Environ Geol 45(3):295–311

Rickenmann D (2005) Hangmuren und Gefahrenbeurteilung. Kurzbericht für das Bundesamt für Wasser und Geologie. Universität für Bodenkultur, Wien, und Eidg. Forschungsanstalt WSL, Birmensdorf

Rymer MJ (1987) The San Salvador earthquake of October 10, 1986—geologic aspects. Earthq Spectra 3(3):435–463

Saaty TL (1977) A scaling method for priorities in hierarchical structures. J Math Psychol 15(3):234–281

Sebesta J (2007) Geomorfología del Área Metropolitana de San Salvador (AMSS) y su relación con los movimientos de ladera. Oficina de Planificación del Área Metropolitana de San Salvador (OPAMSS), San Salvador

Varnes DJ (1978) Slope movement types and processes. In: Schuster RL, Krizek RJ (eds) Landslides: analysis and control. Transportation Research Board, National Research Council, Washington, DC, USA, pp 11–33

Wang F, Sassa K (2007) Landslide simulation by geotechnical model adopting a model for variable apparent friction coefficient. In: Ho K, Li V (eds) 2007 International Forum on Landslide Disaster Management. Geotechnical Division, The Hong Kong Institution of Civil Engineers, Hong Kong, pp 1079–1096

Zapata Martí R, Jovel R (2004) Damages and losses of the 2001 earthquakes in El Salvador. In: Rose WI, Bommer JJ, López DL, Carr MJ, Major JJ (eds) Natural hazards in El Salvador. The Geological Society of America, Boulder, CO, USA, pp 471–480

J. Cepeda (✉)
International Centre for Geohazards, Norwegian Geotechnical Institute (NGI),
Sognsveien 72,
0855 Oslo, Norway
e-mail: jose.cepeda@ngi.no

J. Cepeda
Department of Geosciences, University of Oslo,
P.O.Box 1047 Blindern,
0316 Oslo, Norway

J. A. Chávez
Department of Geotechnics, Faculty of Civil Engineering, Czech Technical University in Prague,
Thákurova 7,
166 29 Praha 6, Czech Republic

C. Cruz Martínez
Oficina de Planificación del Área Metropolitana de San Salvador (OPAMSS),
Diagonal San Carlos, 25 calle poniente y 15 avenida norte, Col. Layco.,
San Salvador, El Salvador